arXiv:nucl-ex/0106004v2 16 Jul 2001

Multiplicity distribution and spectra of negatively charged hadrons in Au+Au collisions at $\sqrt{s_{\rm NN}} = 130$ GeV

C. Adler[11], Z. Ahammed[23], C. Allgower[12], J. Amonett[14], B.D. Anderson[14], M. Anderson[5], G.S. Averichev[9], J. Balewski[12], O. Barannikova[9,23], L.S. Barnby[14], J. Baudot[13], S. Bekele[20], V.V. Belaga[9], R. Bellwied[30], J. Berger[11], H. Bichsel[29], L.C. Bland[12], C.O. Blyth[3], B.E. Bonner[24], R. Bossingham[15], A. Boucham[26], A. Brandin[18], H. Caines[20], M. Calderón de la Barca Sánchez[31], A. Cardenas[23], J. Carroll[15], J. Castillo[26], M. Castro[30], D. Cebra[5], S. Chattopadhyay[30], M.L. Chen[2], Y. Chen[6], S.P. Chernenko[9], M. Cherney[8], A. Chikanian[31], B. Choi[27], W. Christie[2], J.P. Coffin[13], L. Conin[26], T.M. Cormier[30], J.G. Cramer[29], H.J. Crawford[4], M. DeMello[24], W.S. Deng[14], A.A. Derevschikov[22], L. Didenko[2], J.E. Draper[5], V.B. Dunin[9], J.C. Dunlop[31], V. Eckardt[16], L.G. Efimov[9], V. Emelianov[18], J. Engelage[4], G. Eppley[24], B. Erazmus[26], P. Fachini[25], E. Finch[31], Y. Fisyak[2], D. Flierl[11], K.J. Foley[2], J. Fu[15], N. Gagunashvili[9], J. Gans[31], L. Gaudichet[26], M. Germain[13], F. Geurts[24], V. Ghazikhanian[6], J. Grabski[28], O. Grachov[30], D. Greiner[15], V. Grigoriev[18], M. Guedon[13], E. Gushin[18], T.J. Hallman[2], D. Hardtke[15], J.W. Harris[31], M. Heffner[5], S. Heppelmann[21], T. Herston[23], B. Hippolyte[13], A. Hirsch[23], E. Hjort[15], G.W. Hoffmann[27], M. Horsley[31], H.Z. Huang[6], T.J. Humanic[20], H. Hümmler[16], G. Igo[6], A. Ishihara[27], Yu.I. Ivanshin[10], P. Jacobs[15], W.W. Jacobs[12], M. Janik[28], I. Johnson[15], P.G. Jones[3], E. Judd[4], M. Kaneta[15], M. Kaplan[7], D. Keane[14], A. Kisiel[28], J. Klay[5], S.R. Klein[15], A. Klyachko[12], A.S. Konstantinov[22], L. Kotchenda[18], A.D. Kovalenko[9], M. Kramer[19], P. Kravtsov[18], K. Krueger[1], C. Kuhn[13], A.I. Kulikov[9], G.J. Kunde[31], C.L. Kunz[7], R.Kh. Kutuev[10], A.A. Kuznetsov[9], L. Lakehal-Ayat[26], J. Lamas-Valverde[24], M.A.C. Lamont[3], J.M. Landgraf[2], S. Lange[11], C.P. Lansdell[27], B. Lasiuk[31], F. Laue[2], A. Lebedev[2], T. LeCompte[1], R. Lednický[9], V.M. Leontiev[22], P. Leszczynski[28], M.J. LeVine[2], Q. Li[30], Q. Li[15], S.J. Lindenbaum[19], M.A. Lisa[20], T. Ljubicic[2], W.J. Llope[24], G. LoCurto[16], H. Long[6], R.S. Longacre[2], M. Lopez-Noriega[20], W.A. Love[2], D. Lynn[2], R. Majka[31], A. Maliszewski[28], S. Margetis[14], L. Martin[26], J. Marx[15], H.S. Matis[15], Yu.A. Matulenko[22], T.S. McShane[8], F. Meissner[15], Yu. Melnick[22], A. Meschanin[22], M. Messer[2], M.L. Miller[31], Z. Milosevich[7], N.G. Minaev[22], J. Mitchell[24], V.A. Moiseenko[10], D. Moltz[15], C.F. Moore[27], V. Morozov[15], M.M. de Moura[30], M.G. Munhoz[25], G.S. Mutchler[24], J.M. Nelson[3], P. Nevski[2], V.A. Nikitin[10], L.V. Nogach[22], B. Norman[14], S.B. Nurushev[22], G. Odyniec[15], A. Ogawa[21], V. Okorokov[18], M. Oldenburg[16], D. Olson[15], G. Paic[20], S.U. Pandey[30], Y. Panebratsev[9], S.Y. Panitkin[2], A.I. Pavlinov[30], T. Pawlak[28], V. Perevoztchikov[2], W. Peryt[28], V.A Petrov[10], W. Pinganaud[26], E. Platner[24], J. Pluta[28], N. Porile[23], J. Porter[2], A.M. Poskanzer[15], E. Potrebenikova[9], D. Prindle[29],C. Pruneau[30], S. Radomski[28], G. Rai[15], O. Ravel[26], R.L. Ray[27], S.V. Razin[9,12], D. Reichhold[8], J.G. Reid[29], F. Retiere[15], A. Ridiger[18], H.G. Ritter[15], J.B. Roberts[24], O.V. Rogachevski[9], J.L. Romero[5], C. Roy[26], D. Russ[7], V. Rykov[30], I. Sakrejda[15], J. Sandweiss[31], A.C. Saulys[2], I. Savin[10], J. Schambach[27], R.P. Scharenberg[23], K. Schweda[15], N. Schmitz[16], L.S. Schroeder[15], A. Schüttauf[16], J. Seger[8], D. Seliverstov[18], P. Seyboth[16], E. Shahaliev[9], K.E. Shestermanov[22], S.S. Shimanskii[9], V.S. Shvetcov[10], G. Skoro[9], N. Smirnov[31], R. Snellings[15], J. Sowinski[12], H.M. Spinka[1], B. Srivastava[23], E.J. Stephenson[12], R. Stock[11], A. Stolpovsky[30], M. Strikhanov[18], B. Stringfellow[23], H. Stroebele[11], C. Struck[11], A.A.P. Suaide[30], E. Sugarbaker[20], C. Suire[13], M. Šumbera[9], T.J.M. Symons[15], A. Szanto de Toledo[25], P. Szarwas[28], J. Takahashi[25], A.H. Tang[14], J.H. Thomas[15], V. Tikhomirov[18], T.A. Trainor[29], S. Trentalange[6], M. Tokarev[9], M.B. Tonjes[17], V. Trofimov[18], O. Tsai[6], K. Turner[2], T. Ullrich[2], D.G. Underwood[1], G. Van Buren[2], A.M. VanderMolen[17], A. Vanyashin[15], I.M. Vasilevski[10], A.N. Vasiliev[22], S.E. Vigdor[12], S.A. Voloshin[30], F. Wang[23], H. Ward[27], J.W. Watson[14], R. Wells[20], T. Wenaus[2], G.D. Westfall[17], C. Whitten Jr. [6], H. Wieman[15], R. Willson[20], S.W. Wissink[12], R. Witt[14], N. Xu[15], Z. Xu[31], A.E. Yakutin[22], E. Yamamoto[6], J. Yang[6], P. Yepes[24], A. Yokosawa[1], V.I. Yurevich[9], Y.V. Zanevski[9], I. Zborovský[9], W.M. Zhang[14], R. Zoulkarneev[10], A.N. Zubarev[9]

(STAR Collaboration)

[1] *Argonne National Laboratory, Argonne, Illinois 60439*

[2] *Brookhaven National Laboratory, Upton, New York 11973*

[3] *University of Birmingham, Birmingham, United Kingdom*

[4] *University of California, Berkeley, California 94720*

[5] *University of California, Davis, California 95616*

[6] *University of California, Los Angeles, California 90095*

[7] *Carnegie Mellon University, Pittsburgh, Pennsylvania 15213*

[8] *Creighton University, Omaha, Nebraska 68178*

[9] *Laboratory for High Energy (JINR), Dubna, Russia*

[10] *Particle Physics Laboratory (JINR), Dubna, Russia*

[11] *University of Frankfurt, Frankfurt, Germany*

[12] *Indiana University, Bloomington, Indiana 47408*

[13] *Institut de Recherches Subatomiques, Strasbourg, France*
[14] *Kent State University, Kent, Ohio 44242*
[15] *Lawrence Berkeley National Laboratory, Berkeley, California 94720*
[16] *Max-Planck-Institut für Physik, Munich, Germany*
[17] *Michigan State University, East Lansing, Michigan 48824*
[18] *Moscow Engineering Physics Institute, Moscow Russia*
[19] *City College of New York, New York City, New York 10031*
[20] *Ohio State University, Columbus, Ohio 43210*
[21] *Pennsylvania State University, University Park, Pennsylvania 16802*
[22] *Institute of High Energy Physics, Protvino, Russia*
[23] *Purdue University, West Lafayette, Indiana 47907*
[24] *Rice University, Houston, Texas 77251*
[25] *Universidade de Sao Paulo, Sao Paulo, Brazil*
[26] *SUBATECH, Nantes, France*
[27] *University of Texas, Austin, Texas 78712*
[28] *Warsaw University of Technology, Warsaw, Poland*
[29] *University of Washington, Seattle, Washington 98195*
[30] *Wayne State University, Detroit, Michigan 48201*
[31] *Yale University, New Haven, Connecticut 06520*
(February 8, 2008)

The minimum bias multiplicity distribution and the transverse momentum and pseudorapidity distributions for central collisions have been measured for negative hadrons (h^-) in Au+Au interactions at $\sqrt{s_{\rm NN}} = 130$ GeV. The multiplicity density at midrapidity for the 5% most central interactions is $dN_{h^-}/d\eta|_{\eta=0} = 280 \pm 1(\text{stat}) \pm 20(\text{syst})$, an increase per participant of 38% relative to $p\bar{p}$ collisions at the same energy. The mean transverse momentum is 0.508 ± 0.012 GeV/c and is larger than in central Pb+Pb collisions at lower energies. The scaling of the h^- yield per participant is a strong function of $p_\perp$. The pseudorapidity distribution is almost constant within $|\eta| < 1$.

The collision of high energy heavy ions is a promising laboratory for the study of nuclear matter at high energy density and the possible creation and decay of the Quark Gluon Plasma [1]. A new era in the study of high energy nuclear collisions began in the year 2000 with the first operation of the Relativistic Heavy Ion Collider (RHIC) at Brookhaven National Laboratory.

The multiplicity and inclusive single particle transverse momentum ($p_\perp$) distributions of hadrons are important tools for understanding the evolutionary path of the system created in the collision and help to determine the characteristics of the early, hot and dense phase. In this Letter we present the minimum-bias multiplicity distribution and the pseudorapidity (η) and $p_\perp$ distributions for the 5% most central collisions for negative hadrons (h^-) in Au+Au interactions at a center-of-mass energy of $\sqrt{s_{\rm NN}} = 130$ GeV per nucleon pair, measured by the STAR detector at RHIC. The results are compared with reference data from $p\bar{p}$ collisions at a similar energy and collisions of heavy nuclei at a lower energy.

The main tracking detector for STAR is a large Time Projection Chamber (TPC), which measures charged particles in the pseudorapidity range $|\eta| < 1.8$ with complete azimuthal acceptance. It is placed inside a uniform solenoidal magnetic field of strength 0.25 T. The trigger detectors are an array of scintillator slats (CTB) arranged in a barrel surrounding the TPC, and two hadronic calorimeters (ZDCs) at ± 18 m from the detector center and at zero degrees relative to the beam axis. The ZDCs intercept spectator neutrons from the collision and provide a measure of the collision centrality. Further details on the apparatus can be found in [2].

During the Summer 2000 run, RHIC delivered collisions between Au nuclei at $\sqrt{s_{\rm NN}} = 130$ GeV. The data presented here are from a minimum-bias sample, triggered by a coincidence of signals above threshold in both ZDCs with the RHIC beam crossing. The ZDC threshold was set to ensure efficient detection of single spectator neutrons. The efficiency of the ZDC coincidence trigger for central events was measured using a high-threshold CTB trigger. The trigger efficiency was found to be above 99% for the entire range of multiplicities reported in this Letter.

The offline reconstruction found a primary vertex for each event by propagating the measured tracks through the field towards the beamline. The vertex resolution for high multiplicity events is approximately 150 μm, both perpendicular and parallel to the beam axis. Events used in the analysis have a vertex within ± 95 cm of the center of the TPC along the beam axis. The vertex finding efficiency is 100% for events with more than 50 primary tracks in the TPC acceptance, decreasing to 60% for those with fewer than 5 primary tracks. 60,000 minimum-bias Au+Au events were used for this analysis.

Particle production was studied through the yield of primary negative hadrons, comprising mostly π^- with an admixture of K^- and $\bar{p}$. The h^- distribution includes the products of strong and electromagnetic decays. Negatively charged hadrons were studied in order to exclude effects due to participant nucleons. Charged particle tracks reconstructed in the TPC were accepted for this analysis if they fulfilled requirements on number of points on the track and on pointing accuracy to the event vertex. The measured raw distributions were corrected for acceptance, track reconstruction efficiency, and contamination due to interactions in material, misidentified non-hadrons, and the products of weak decays. The reconstruction efficiency was determined by embedding simulated tracks into real events at the raw data level, reconstructing the full events, and comparing the simulated input to the reconstructed output. This technique requires a precise simulation of isolated single tracks, achieved by a detailed simulation of the STAR apparatus based on GEANT [3] and a microscopic simulation of the TPC response. The multiplicity of the embedded tracks was limited to 5% of the multiplicity of the real event in the same phase space as the simulated data, thereby perturbing the real event at a level below the statistical fluctuations within the event sample.

The acceptance is on average 95% for tracks within the fiducial volume having $p_\perp > 300$ MeV/c. The tracking efficiency ranges between 70%–95%, depending on $p_\perp$ and the multiplicity of the event. For tracks with $p_\perp > 200$ MeV/c the efficiency is above 85%. Accepted tracks for this analysis have $0.1 < p_\perp < 2$ GeV/c and $|\eta| < 1.0$.

Instrumental backgrounds due to photon conversions and secondary interactions with detector material were estimated using the detector response simulations mentioned above, together with events generated by the HIJING model [4]. The simulations were calibrated using data in regions where background processes could be directly identified. The measured yield also contains contributions from the products of weak decays, primarily K^0_S, that were incorrectly reconstructed as primary tracks. The background fraction of the raw signal is approximately 20% at $p_\perp = 100$ MeV/c, decreasing with increasing $p_\perp$. The average fraction of background tracks in the uncorrected sample is 7%. All corrections were calculated as a function of the uncorrected event multiplicity. The systematic uncertainty due to the corrections was estimated by studying the variation in the final spectra due to both a large variation in the track quality cuts with corresponding recalculation of the correction factors, and a small variation in the track quality cuts with no adjustment of the correction factors.

Figure 1 shows the corrected, normalized multiplicity distribution within $|\eta| < 0.5$ and $p_\perp > 100$ MeV/c for minimum bias Au+Au collisions. The data were normalized assuming a total hadronic inelastic cross section of 7.2 barn for Au+Au collisions at $\sqrt{s_{\rm NN}} = 130$ GeV, derived from Glauber model calculations [5]. The multiplicity bin below $N_{h^-} = 5$ is not shown, due to large systematic uncertainties in the vertex reconstruction efficiency and large background contamination. Its relative contribution to the total cross section was estimated to be 21% by normalizing the HIJING multiplicity distribution to the measured data in the region $5 < N_{h^-} < 25$. This procedure relies on the assumption that very peripheral interactions are well described by the superposition of a few nucleon-nucleon collisions in the geometry of a nuclear collision, and can therefore be accurately modelled by HIJING. The systematic error on the vertical scale is estimated to be 10% and is dominated by uncertainties in the total hadronic cross section and the relative contribution of the first bin. The systematic error on the horizontal scale is 6% for the entire range of multiplicity and is depicted by horizontal error bars on a few data points only.

The shape of the h^- multiplicity distribution is dominated over much of the N_{h^-} range by the nucleus-nucleus collision geometry, consistent with findings at lower energies. However, the shape of the tail region at large N_{h^-} is determined by fluctuations and acceptance. These overall features are also observed in the HIJING calculation, shown as histogram in Fig. 1. The distribution for the 5% most central collisions (360 mb), defined using ZDC coincidence, is shown as the shaded area in Fig. 1.

Figure 2, upper panel, shows the transverse momentum distribution of negatively charged hadrons for central Au+Au collisions at midrapidity ($|\eta| < 0.1$) within $0.1 < p_\perp < 2$ GeV/c. Statistical errors are smaller than the symbols. The correlated systematic error is estimated to be below 6%. The data are fit in the range $0.2 < p_\perp < 2$ GeV/c by a QCD inspired power-law function of the form $d^2N_{h^-}/dp_\perp^2 d\eta = A\,(1 + p_\perp/p_0)^{-n}$ where A, n, and p_0 are free parameters. The upper panel of Fig. 2 also shows the $p_\perp$-distributions of negatively charged hadrons for central Pb+Pb collisions at $\sqrt{s_{\rm NN}} = 17$ GeV from NA49 [6] and for minimum-bias $p\bar{p}$ collisions at $\sqrt{s} = 200$ GeV from UA1 [7], fitted with the same function. The NA49 distribution, which was reported in units of pion rapidity, was transformed to units of pseudorapidity. The UA1 invariant cross section $Ed^3\sigma/d^3p$ reported in Ref. [7] was scaled by $2\pi/\sigma_{\rm inel}$, where $\sigma_{\rm inel} = 42$ mb [8]. The power law fits all three datasets well. The mean $p_\perp$ can be derived from the fit parameters as $\langle p_\perp \rangle = 2p_0/(n-3)$. The fit to the STAR data gives $p_0 = 3.0 \pm 0.3$ GeV/c, $n = 14.8 \pm 1.2$, and $\langle p_\perp \rangle = 0.508 \pm 0.012$ GeV/c. The strong correlation of fit parameters p_0 and n must be taken into account when calculating the error on $\langle p_\perp \rangle$. The $\langle p_\perp \rangle$ from STAR is larger than that from both central collisions of heavy nuclei at much lower energy ($\langle p_\perp \rangle_{\rm NA49} \simeq 0.429$ GeV/c [9]) and nucleon-nucleon collisions at a comparable energy ($\langle p_\perp \rangle_{\rm UA1} = 0.392 \pm 0.003$ GeV/c).

The PHENIX collaboration has reported that $\langle E_\perp \rangle / \langle N_{ch} \rangle$ for central collisions of heavy nuclei is constant between SPS and RHIC energies, with a value of ~ 0.8 GeV [10]. Under the assumption that the particle composition does not change significantly between the SPS and RHIC, this finding is in apparent disagreement with the above observation that $\langle p_\perp \rangle$ increases by 18%. It should be noted, however, that the systematic error on the SPS measurement of $\langle E_\perp \rangle / \langle N_{ch} \rangle$ is 20% [11], so that these results are consistent within errors.

Figure 2, lower panel, shows the ratio of the STAR and UA1 $p_\perp$-distributions. Since the UA1 distribution is measured at $\sqrt{s} = 200$ GeV, $d\sigma/dp_\perp$ is scaled by two factors for quantitative comparison to the STAR data at 130 GeV: *(i)* $R(130/200)$, the $p_\perp$-dependent ratio of invariant cross sections for charged particle production in $p\bar{p}$ collisions at $\sqrt{s} = 130$ and 200 GeV, and *(ii)* $\mathrm{T_{AA}} = 26 \pm 2$ mb^{-1}, the nuclear overlap integral [12] for the 5% most central Au+Au collisions. R varies from 0.92 at $p_\perp = 0.2$ GeV/c to 0.70 at $p_\perp = 2.0$ GeV/c, and was derived using scaling laws for $\langle p_\perp \rangle$ and $dN_{\mathrm{ch}}/d\eta$ as a function of $\sqrt{s}$ [7,13] together with the extrapolation to 130 GeV of power-law parameterizations at $\sqrt{s} = 200$–900 GeV [7]. The shaded boxes show the total error of the ratio, which is the linear sum of the errors of the measured data, depicted by the error bars, and the systematic error due to uncertainties in the scaling with $\mathrm{T_{AA}}$ and R.

There are two simple predictions for the scaled ratio. In lower energy hadronic and nuclear collisions, the total pion yield due to soft (low $p_\perp$) processes scales as the number of participants ("wounded" nucleons) in the collision (e.g. [6,14]). The scaled ratio in this case is 0.164, assuming 172 participant pairs [15] and a mean number of binary collisions of 1050 ($= \sigma_{\mathrm{inel}} \mathrm{T_{AA}}$, where for $\sqrt{s} = 130\,\mathrm{GeV}$ $\sigma_{\mathrm{inel}} \simeq 40.5$ mb [8]) for the 5% most central Au+Au events. In contrast, if hadron production is due to hard (high $p_\perp$) processes and there are no nuclear-specific effects (see below), the hadron yield will scale as the number of binary nucleon-nucleon interactions in the nuclear collision and the value of the ratio is unity. There are important nuclear effects which may alter the scaling as a function of $p_\perp$ from these simple predictions, including initial state multiple scattering [16], shadowing [17], jet quenching [18], and radial flow [19]. The scaled ratio exhibits a strong $p_\perp$ dependence, rising monotonically with increasing $p_\perp$ from Wounded Nucleon scaling at low $p_\perp$ but not reaching Binary Collision scaling at the highest $p_\perp$ reported. This is consistent with the presence of radial flow, as well as the onset of hard scattering contributions and initial state multiple scattering with rising $p_\perp$.

Figure 3 shows the normalized pseudorapidity distribution of h^- for the 5% most central collisions within $|\eta| < 1.0$, both for $p_\perp > 100$ MeV/c and for all $p_\perp$. The latter was obtained by fitting a power-law function in the range $0.1 < p_\perp < 2$ GeV/c and extrapolating to $p_\perp = 0$ in order to estimate the content of the first bin. The error bars indicate the uncorrelated systematic errors. The statistical errors are negligible. The correlated systematic error applied to the overall normalization is estimated to be below 6% for $p_\perp > 100$ MeV/c and 7% for all $p_\perp$.

The η distribution is almost constant within $|\eta| < 1$, exhibiting a small rise at larger η. This shape is expected from a boost invariant source (i.e., constant in rapidity), taking into account the transformation from y to η. It should be noted that in Pb+Pb collisions at $\sqrt{s_{\mathrm{NN}}} = 17$ GeV the pseudo-rapidity distribution of charged hadrons [20] and the rapidity distribution of negative hadrons (assuming the pion mass) [6] were found to peak at midrapidity, suggesting a significant change in the longitudinal phase space distribution between the SPS and RHIC. Measurement of the rapidity distribution of identified particles is needed to establish the boost invariance at RHIC.

The h^- density at midrapidity for $p_\perp > 100\,\mathrm{MeV}/c$ is $dN/d\eta|_{\eta=0} = 261 \pm 1(\mathrm{stat}) \pm 17(\mathrm{syst})$. Extrapolation to $p_\perp = 0$ yields $dN/d\eta|_{\eta=0} = 280 \pm 1(\mathrm{stat}) \pm 20(\mathrm{syst})$. Assuming an average of 172 participant pairs per central Au+Au collision, this corresponds to $1.63 \pm 0.12\,h^-$ per participant nucleon pair per unit pseudorapidity, a 38% increase over the yield in $p\bar{p}$ collisions extrapolated to the same energy [21] (we neglect isospin correction factors of order 1–3%) and a 52% increase over Pb+Pb collisions at $\sqrt{s_{\mathrm{NN}}} = 17$ GeV [6].

For the total charged multiplicity density in Au+Au interactions at $\sqrt{s_{\mathrm{NN}}} = 130$ GeV, the PHOBOS collaboration has reported $dN_{ch}/d\eta|_{|\eta|<1} = 555 \pm 12(\mathrm{stat}) \pm 35(\mathrm{syst})$ (6% most central collisions) [22], while the PHENIX collaboration has reported $dN_{ch}/d\eta|_{\eta=0} = 622 \pm 1(\mathrm{stat}) \pm 41(\mathrm{syst})$ (5% most central) [23]. To compare to these results, positive charged particles were analysed in the framework described above. For the 5% most central collisions, STAR measures a total charged multiplicity density of $dN_{ch}/d\eta|_{\eta=0} = 567 \pm 1(\mathrm{stat}) \pm 38(\mathrm{syst})$.

In conclusion, we find that particle production per participant in central Au+Au collisions at $\sqrt{s_{\mathrm{NN}}} = 130$ GeV increases by 38% relative to $p\bar{p}$ and 52% compared to nuclear collisions at $\sqrt{s_{\mathrm{NN}}} = 17$ GeV. The $p_\perp$ distribution is harder than that of the $p\bar{p}$ reference system for the $p_\perp$ region up to 2 GeV/c. Scaling of produced particle yield with number of participants shows a strong dependence on $p_\perp$, with Wounded Nucleon scaling achieved only at the lowest measured $p_\perp$. The h^- pseudorapidity distribution is almost constant within $|\eta| < 1$.

Acknowledgments: We wish to thank the RHIC Operations Group at Brookhaven National Laboratory for their tremendous support. This work was supported by the Division of Nuclear Physics and the Division of High Energy Physics of the Office of Science of the U.S.Department of Energy, the United States National Science Founda-

tion, the Bundesministerium fuer Bildung und Forschung of Germany, the Institut National de la Physique Nucleaire et de la Physique des Particules of France, the United Kingdom Engineering and Physical Sciences Research Council, Fundacao de Amparo a Pesquisa do Estado de Sao Paulo, Brazil, and the Russian Ministry of Science and Technology.

[1] J.-P. Blaizot, Nucl. Phys. A **661**, 3c (1999).
[2] K.H. Ackermann *et al.*, Nucl. Phys. A **661**, 681c (1999).
[3] P. Nevski, in *Proceedings of International Conference on Computing in High Energy and Nuclear Physics*, Padova, Italy, 2000, A212, http://chep2000.pd.infn.it/-abst/abs_a212.htm.
[4] X.N. Wang and M. Gyulassy, Phys. Rev. D **44**, 3501 (1991); Comput. Phys. Commun. **83**, 307 (1994). We used HIJING 1.35 with standard parameter settings.
[5] A.J. Baltz, C. Chasman, and S.N. White, Nucl. Instr. Meth. A **417**, 1 (1998).
[6] H. Appelshäuser *et al.*, Phys. Rev. Lett. **82**, 2471 (1999).
[7] C. Albajar *et al.*, Nucl. Phys. B **335**, 261 (1990).
[8] G.J. Alner *et al.*, Z. Phys. C **32**, 153 (1986).
[9] This value results from a power law fit to $1/p_\perp\, d^2N/dp_\perp d\eta$ and differs from the value derived within a fixed pion rapidity window of $\langle p_\perp \rangle = 385 \pm 18$ MeV/c reported in [6].
[10] K. Adcox *et al.*, nucl-ex/0104015 (2001).
[11] M.M. Aggarwal *et al.*, Eur. Phys. J. C 18, 651 (2001).
[12] K. J. Eskola, K. Kajantie, and J. Lindfors, Nucl. Phys. B **323**, 37 (1989).
[13] D.E. Groom *et al.*, Eur. Phys. J. C **15**, 1 (2000).
[14] A. Bialas, M. Bleszynski, and W. Czyz; Nucl. Phys. B **111**, 461 (1976).
[15] D. Kharzeev and M. Nardi, Phys. Lett. B **507**, 121 (2001).
[16] D. Antreasyan *et al.*, Phys. Rev. D **19**, 764 (1979).
[17] V. Emel'yanov *et al.*, Phys. Rev. C **61**, 044904 (2000).
[18] X.N. Wang and M. Gyulassy, Phys. Rev. Lett. **68**, 1480 (1992); X.N. Wang, Phys. Rev. C **58**, 2321 (1998).
[19] E. Schnedermann, J. Sollfrank, and U. Heinz, Phys. Rev. C **48**, 2462 (1993).
[20] G. Agakichiev *et al.*, Nucl. Phys. A **638**, 467c (1998).
[21] G.J. Alner *et al.*, Z. Phys. C **33**, 1 (1986).
[22] B.B. Back *et al.*, Phys. Rev. Lett. **85**, 3100 (2000).
[23] K. Adcox *et al.*, Phys. Rev. Lett. **86**, 3500 (2001).

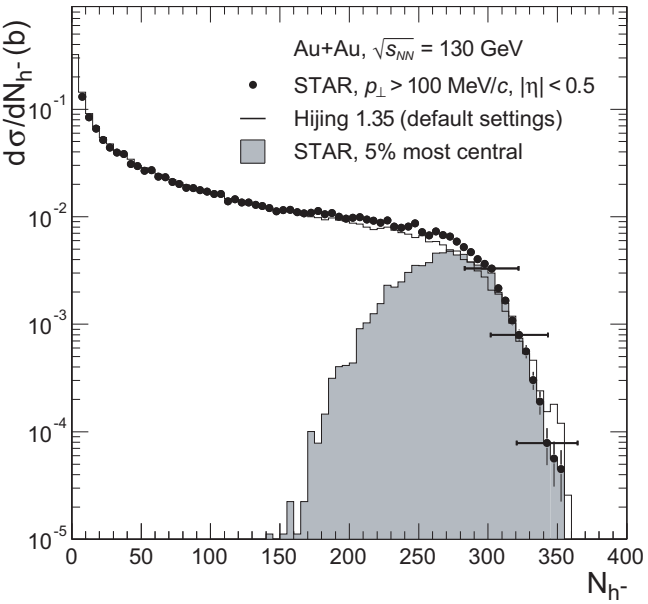

FIG. 1. Normalized multiplicity distribution of h^- with $p_\perp > 100$ MeV/c in Au+Au collisions at $\sqrt{s_{\rm NN}} = 130$ GeV. The shaded area is 5% most central collisions, selected by ZDC coincidence. The solid curve is the prediction from the HIJING model.

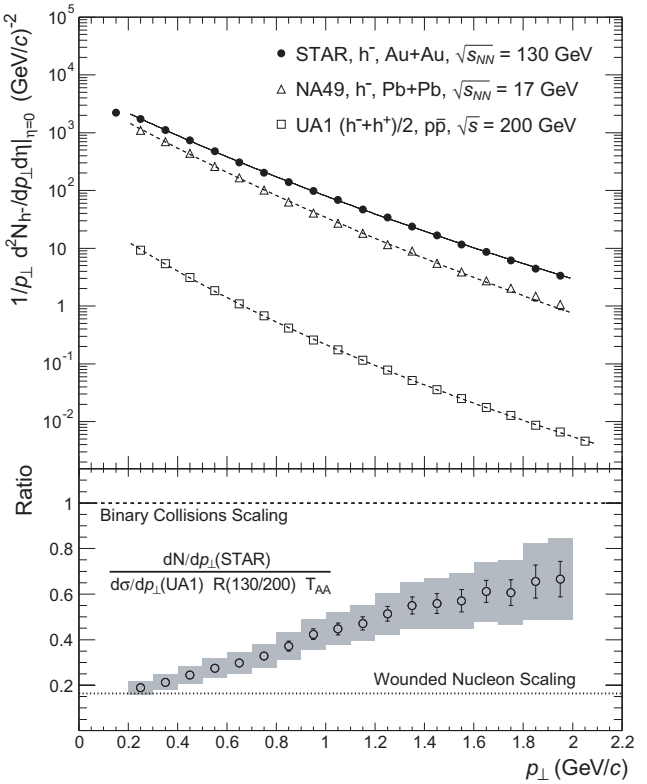

FIG. 2. Upper panel: h^- $p_\perp$-spectra for the 5% most central Au+Au collisions at midrapidity ($|\eta| < 0.1$) for several systems. The curves are power-law fits to the data. Lower panel: ratio of STAR and scaled UA1 $p_\perp$-distributions (see text).

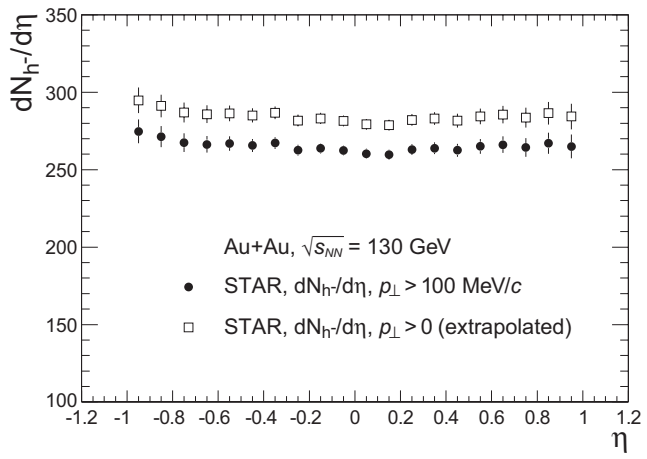

FIG. 3. h^- pseudorapidity distribution from 5% most central Au+Au collisions for $p_\perp > 100$ MeV/c (filled circles) and all $p_\perp$ (open squares).